Journal of Hazardous Materials, 16 (1987) 357–380
Elsevier Science Publishers B.V., Amsterdam — Printed in The Netherlands

THE EFFECT OF INITIAL POTENTIAL ENERGY ON THE DILUTION OF A HEAVY GAS CLOUD

D.M. WEBBER and C.J. WHEATLEY

Safety and Reliability Directorate, Wigshaw Lane, Culcheth, Warrington, Cheshire WA3 4NE (Great Britain)

(Received October 22, 1986; accepted February 16, 1987)

Summary

A model is presented for the behaviour of an instantaneously released heavy gas cloud in calm conditions, or sufficiently close to the source that gravity effects dominate ambient turbulence effects. The object of this model is to clarify how turbulence generated from the initial potential energy of the cloud may effect the subsequent dilution.

The model is an integral one which treats the turbulent energy in the cloud as a dynamic variable which determines the entrainment rate. It is constructured such that overall dissipation of mechanical energy is guaranteed. The turbulent energy of the cloud released from rest is thus generated explicitly from the initial potential energy, and the entrainment rate may depend on the initial aspect (height to radius) ratio, and the initial density, of the cloud. An investigation of the properties of the model indicates that these effects, whilst present, are small.

Consequently, this more detailed study of the energy budget of the cloud, lends considerable support to simple models which treat the early dilution of the cloud as "edge entrainment" with an entrainment velocity proportional to the spreading rate.

1. Introduction

The Thorney Island trials have provided an extensive data base which will aid enormously the development of mathematical models for use in hazard analysis. Indeed, the experiments were designed [1,2] not only to improve our general understanding of heavy gas dispersion, but also to distinguish between the predictions of a profusion of existing models. (See Refs. [3–5] for a review and in particular Figs. 10.2–10.5 of Ref. [1].)

The broad features of the data lend support to a class of models wherein the cloud is pictured as a right cylinder of radius R, volume V and average depth

$$H=\frac{V}{\pi R^2} \tag{1.1}$$

and evolving according to equations of the form

0304-3894/87/$03.50

$$\frac{dR}{dt} = U_f \tag{1.2}$$

$$\frac{dV}{dt} = (2\pi RH)\,U_E + (\pi R^2)\,U_T \tag{1.3}$$

where the spreading velocity U_f, and the top* and edge* entrainment velocities U_T and U_E, as well as the downwind advection velocity are modelled in terms of the geometric variables R, V, H and the relative density excess

$$\Delta' = (\rho - \rho_a)/\rho_a \tag{1.4}$$

As the entrainment process involves isothermal mixing of inert gases, the buoyancy parameter

$$b = \frac{g}{\pi}\Delta' V \tag{1.5}$$

must be conserved, and the mean concentration is inversely proportional to the volume V.

The trials give considerable information about the various velocity parameters of such a model. In particular

$$U_f = 1.07\ (g\Delta' H)^{1/2} \tag{1.6}$$

is a good representation [6,7] of the observed spreading velocity in the early stages (but after the short period of radial acceleration). The widely adopted edge entrainment model

$$U_E = \alpha_E U_f \tag{1.7}$$

is consistent with the data [8] for $\alpha_E \approx 0.7$. These are also consistent with earlier, smaller scale trials [9].

In many models of this type [3–5] the top entrainment velocity U_T is modelled in terms of the ambient atmospheric turbulence and the gravitational stability of the cloud, and for initially dense clouds its effect is negligible compared to that of U_E until the cloud has diluted sufficiently or until the cloud top area has become sufficiently large. Again the Thorney Island data are consistent with such ideas depending on the model for U_T.

Thus the prospects for this type of simple box model look good, in so far as the Thorney Island data go. However, the trials were all performed at a similar

*We shall adhere to the common practice of referring to these terms as edge and top entrainment. While, however, the form of eqn. (1.3) is suggestive of entrainment through the edge and top, the simple box model cannot provide any direct insight into where the entrainment actually takes place. It may in fact, be better to think of these terms as gravity-powered and wind-powered entrainment, respectively.

high initial aspect ratio ($H_0/R_0=1$) and almost all with very similar density excess ($\Delta_0'=1$)*. In fact both the initial potential energy of the cloud and the deduced value of the edge entrainment coefficient α_E (which can only lie between 0 and 1) are 'large'. Given that the edge entrainment model is essentially one of gravity-powered entrainment, it may be reasonable then to conjecture that these observations are related, and that α_E may in general depend on H_0/R_0 and on Δ_0'. We shall investigate this question here in the framework of an integral model. Because we are interested in the gravity dominated, "edge entraining" phase, we shall consider a very dense cloud or, equivalently, very calm atmospheric conditions.

The two principal ideas behind our approach are that entrainment is related to the level of turbulence within the medium into which it takes place, and that the turbulence intensity in a cloud spreading from rest in a calm atmosphere is determined by its initial potential energy. We shall therefore present a model based on the energy budget of the cloud and examine its solution in order to draw conclusions about the entrainment rate.

2. The energy budget of the cloud

Consider a cloud released instantaneously at ambient temperature into calm air. Let the mean kinetic energy associated with the radial expansion of the cloud be T; let the potential energy of the cloud be P, and the turbulent kinetic energy within the cloud be K. The energy budget is schematically:

$$\begin{aligned}
\frac{dT}{dt} &= \Gamma-\Omega-\Pi \\
\frac{dP}{dt} &= -\Gamma \qquad +I \\
\frac{dK}{dt} &= \qquad \Pi-I-D \\
\hline
\frac{dE}{dt} &= \quad -\Omega \qquad -D
\end{aligned} \tag{2.1}$$

Here Γ is the rate at which gravity converts potential energy into kinetic, Ω is the rate at which the cloud does work on the surrounding air, Π is the rate of turbulent energy production, I is the rate of increase of potential energy due to entrainment**, and D is the rate of dissipation of turbulent kinetic energy into

*The philosophy guiding the design of the trials was to obtain a high quality data set covering a limited region of the parameter space, rather than to spread effort more thinly.

**This increase arises when the entrained air is mixed with the gas already in the cloud.

heat*. Γ, Ω, Π, I, and D are all greater than or equal to zero. This guarantees that the total energy

$$E = T + P + K \tag{2.2}$$

is dissipated.

The gravity spreading term Γ and the work term Ω have their counterpart in most existing box models (see Refs. [3–5]) and are relatively well understood phenomenologically for self-similar radial spread. Because we are interested in the way the initial potential energy is converted to kinetic and turbulent energy, we shall also model these terms in the initial, radially accelerating phase.

To model entrainment in the framework of eqn. (2.1) the entrainment term I must be modelled in terms of the turbulence level K. It is convenient to do this via the familiar concept of an entrainment velocity. The turbulence is modelled in terms of the production rate Π and dissipation rate D. The entrainment rate depends implicitly on these via the turbulent energy K. Such a model constitutes on integral version of a turbulence closure scheme.

3. A model for a cloud in calm conditions

3.1 Entrainment

Let us write the entrainment equation as

$$\frac{\mathrm{d}V}{\mathrm{d}T} = W \pi R^2 \tag{3.1}$$

where W is an entrainment velocity. This is consistent with the idea that even "edge" entrainment appears to take place in an annular region on top of the cloud behind the head [10]. (But eqn. (3.1) reduces to eqn. (1.3) if one writes $W = U_T + 2HU_E/R$.)

Further, let us model the entrainment rate as

$$W = \frac{\alpha_T \sqrt{k}}{(Ri)^{\mu}} \tag{3.2}$$

where

$$k = \frac{K}{\rho V} \tag{3.3}$$

*Note that whilst we have not mentioned direct dissipation of mean kinetic energy T into heat, or transport of turbulent energy out of the cloud, these phenomena can be incorporated into eqn. (2.1) simply by redefinitions of Π and D. Since these effects are not expected to dominate, and our models of Π and D will in any case contain free parameters, we shall not consider them further here.

is the mean specific turbulent energy of the cloud, and

$$Ri=\frac{g\Delta' H}{k} \tag{3.4}$$

is a bulk Richardson number*. α_T and μ are dimensionless constants. Equation (3.2) is consistent with widely accepted ideas (see [3] for a review) of suppression of entrainment across a stable density interface. (However, owing to the different turbulence production mechanism, there is no reason to suppose that α_T or μ should be similar to values found in experiments where the entrainment is not associated with an advancing gravity front.)

The entrainment model is completed by the observation that for isothermal flows (such as the Thorney Island trials) entrainment must conserve the buoyancy variable

$$b=\frac{1}{\pi} g\Delta' V \tag{3.5}$$

3.2 Spreading

The usual spreading law eqn. (1.2) is a good approximation to what is observed in a quasi-steady situation. It does not model the initial radial acceleration of a cloud released from rest. It is essential to model this phase in order to derive the energy budget of the cloud in terms of the initial potential energy. To do this we introduce a shape factor s (see also Refs. [3,11,12]) such that the height of the cloud at the front is Hs. Thus if s is larger than 1 then, from eqn. (1.1), the cloud has a concave top.

Balancing the hydrostatic pressure drop across the front of the cloud with an air resistance pressure proportional to $\rho_a U^2$ gives the radial behaviour

$$\frac{dR}{dt}=U \tag{3.6}$$

with

$$U=\kappa(g\Delta' Hs)^{1/2} \tag{3.7}$$

The distribution of gas within the cloud and hence the shape factor s is governed by the radial momentum equation of the flow. We shall approximate (the integral of) this by

$$\rho\frac{dU}{dt}+\rho_a\frac{WU}{H}=\frac{4g(\rho-\rho_a)(1-s)H}{R}-\frac{C\rho U\sqrt{k}}{H} \tag{3.8}$$

*Of course eqn. (3.2) cannot be valid down to very small values of Ri. We shall see, however, that Ri (thus defined) achieves a minimum value at some finite time and thereafter increases (in absolutely calm conditions). For current purposes, then eqn. (3.2) should be adequately although it might require modification should one wish to take the model further.

The left-hand side of this equation is just $V^{-1}(\mathrm{d}/\mathrm{d}t)\rho VU$. We have assumed that the radial momentum of the cloud (proportional to ρVU) is unaffected by entrainment, and hence the right-hand side is independent of W. The first term on the right is the gravity driving term and is found from a self-similar solution [12] of the shallow layer equations appropriate in the inviscid, zero-entrainment limit. For $s<1$ (a cloud thinner at the edge than in the middle) the gravity term acts to throw material outwards; for $s>1$ (a cloud with a raised edge) it pulls material inwards. The final term on the right represents the effects of friction with the ground. C is a friction coefficient.

In the model presented here s may increase from zero as the cloud accelerates radially from rest. The simple spreading behaviour of eqn. (1.3) will arise if s is constant and the flow is self-similar. It is possible [3] that the front condition eqn. (3.7) should be modified when the flow is not self-similar. It is not, however, necessary to do this to obtain the desired effect of a transfer of potential to kinetic energy. Furthermore such a modification has no effect at large time. We therefore use eqn. (3.7), which we assume to be a sufficiently good approximation if the free parameter κ is optimised.

It is also possible that eqn. (3.8), being derived from shallow layer theory, will not give a quantitative fit to data in the deep cloud régime. Our primary motivation is to include the desired effects in a simple way, in order to render an analytic approach as tractable as possible and gain an understanding of the dilution mechanisms. Equations (3.7) and (3.8) give simple description of a cloud spreading radially allowing both radial acceleration and deceleration in a way which should be fairly accurate at low aspect ratio and qualitatively correct at higher aspect ratio. We shall discuss the nature of "deep cloud" corrections in Section 4.7.

3.3 Turbulence

Equations (3.1–3.8) together with the definitions

$$H=\frac{V}{\pi R^2} \tag{3.9}$$

and

$$\Delta' = (\rho-\rho_a)/\rho_a \tag{3.10}$$

from Section 1 comprise ten equations for the eleven variables R, V, H, U, s, W, K, k, Ri, ρ, and Δ'. It remains to close the system of equations with a model for the turbulent energy K. In the interests of clarity let us write down our model for K and then discuss the derivation. The proposed equation is

$$\frac{dK}{dt}=\alpha_f\frac{\pi b\rho_a UHs^2}{R}+\frac{\xi_1}{4}\rho_a\frac{U^2WV}{H}+\frac{\xi_2}{2}\frac{C\rho VU^2\sqrt{k}}{H}$$

$$-\frac{\pi}{2}\rho_a bW-\alpha_D\frac{\rho Vk^{3/2}}{H} \qquad (3.11)$$

PRODUCTION — BUOYANT DESTRUCTION — DISSIPATION

where α_f, α_D, ξ_1, and ξ_2 are dimensionless constants.

The dissipation term in eqn. (3.11) is the term "D" of eqn. (2.1). It simply corresponds to the assumption of a specific dissipation rate proportional to $k^{3/2}/H$.

The buoyant destruction term corresponds to "Γ" in eqn. (2.1). This has been derived by estimating the potential energy of the cloud to be

$$P=\tfrac{1}{2}g\rho_a\Delta' VH \qquad (3.12)$$

It follows that

$$\frac{dP}{dt}=-\pi b\rho_a\frac{UH}{R}+\frac{\pi}{2}\rho_a bW \qquad (3.13)$$

The two terms on the right of eqn. (3.13) correspond exactly to "$-\Gamma$" and "Γ" of eqn. (2.1), and hence the second term gives the buoyant destruction rate in eqn. (3.11).

The three production terms of eqn. (3.11) correspond (in toto) to the term "Π" in eqn. (2.1). The first represents the rate of production at the front, which is modelled as a fraction α_f of the rate of doing work, which is $[\tfrac{1}{2}g\rho_a\Delta' Hs][2\pi RHs]U$.

The other production terms cover the whole area of the cloud. They are inferred from eqn. (3.8) which implies

$$\frac{d}{dt}(\tfrac{1}{4}\rho VU^2)=2\pi b\rho_a(1-s)\frac{HU}{R}-\rho_a\frac{VU^2W}{4H}-\frac{C\rho VU^2\sqrt{k}}{2H} \qquad (3.14)$$

This constitutes an approximate* kinetic energy equation. The first term on the right includes gravity and front resistance effects. The second term represents the loss of mean kinetic energy in mixing with the ambient air, and the third the loss by friction with the ground.

The loss of energy given by these last two terms is assumed to occur by shear production of turbulent energy which is then dissipated. Thus they contribute to the production term "Π" of eqn. (2.1). In eqn. (3.11) they are introduced

*A total kinetic energy of $\frac{1}{4}\rho VU^2$ is found for a cylindrical cloud with velocity field $U(r)=Ur/R$ for $0\leqslant r\leqslant R$. If the cloud deviates from this idealisation (in shape or velocity field) then eqn. (3.14) may be regarded as an approximation to the kinetic energy equation.

with coefficients ξ_1, ξ_2 of order 1, which are to allow for uncertainties in estimating the mean kinetic energy via eqn. (3.14). For example, the mean (non-turbulent) kinetic energy of the cloud includes a part due to the height-averaged flow and a part due to the "rolling" motion (seen clearly at the front in, for example, the Thorney Island trials), which is too regular to be considered as turbulence. We have assumed that both of these are of order ρVU^2. Uncertainty in the amount of energy in this rolling motion is thus translated into uncertainty in the precise values of α_f, ξ_1, and ξ_2.

Equations (3.1–3.11) now form a closed set for eleven variables. These are not precisely of the structure of eqn. (2.1) but, as we have seen, that structure has been used in the derivation of the turbulence equation (3.11).

3.4 Solution of the model

The model presented in eqns. (3.1–3.11) is not exactly soluble. We shall present approximate, analytic solutions valid in the large time limit. We shall see that the case $\mu < 1$ differs significantly from that with $\mu \leqslant 1$. A numerical solution will be presented for the case $\mu = 1$, and examined in the light of data from the Thorney Island trials. The asymptotic analytic solutions will be compared with simple edge-entrainment models.

4. Analysis of the model

4.1 Spreading régimes

By analogy with a spreading pool [11,12] we expect up to three spreading régimes: an initial régime in which radial acceleration effects are important; an intermediate régime which is described by the simpler ideas of Section 1 (with $R \sim \sqrt{t}$); and a late time régime in which friction effects become important resulting in a collapse of the gravity head and a breakdown of the $R \sim \sqrt{t}$ spreading law*. We are primarily interested in the first two of these, and it therefore simplifies the analysis considerably if we set $C = 0$ for the remainder of this work. Thus when we refer to "asymptotically large" time in the following sections it should be interpreted as large enough that the effects of the initial régime are unimportant but not so large that friction effects become significant**.

4.2 The large time behaviour of the solution

We shall give here the asymptotic (large time) behaviour of the ($C = 0$) solution. It can be verified straightforwardly (if a little tediously) by substi-

*This may also be expected owing to turbulence in the atmosphere in all but absolutely calm conditions.

**The clear $R \sim \sqrt{t}$ spreading régime observed in the Thorney Island trials [6] can be taken as evidence that $C = 0$ is a good approximation for a considerable time; in general we expect $C = O(10^{-3})$ which will mean a very late onset of the importance of friction terms.

tuting these expressions into the equations of Section 3. We shall assume the Boussinesq approximation, $\Delta' \ll 1$, is valid. (This is actually only guaranteed asymptotically if $\mu \leqslant 1$, as we shall see.) The large time ($t \to \infty, R \to \infty$) spreading behaviour is given by

$$U = \frac{p\sqrt{b}}{R} \quad (= p\sqrt{g\Delta' H}) \tag{4.1}$$

where b is the buoyancy parameter defined in eqn. (3.5) and p is a dimensionless constant. This implies

$$R^2 = 2pb^{1/2}t \tag{4.2}$$

The cloud dilution is given by

$$\left.\begin{aligned} \left(\frac{V}{V_0}\right) &= \tilde{\beta}\left(\frac{R}{R_0}\right)^{2\alpha} && ;\mu \leqslant 1 \\ &= \tilde{\beta}\left\{1 - \frac{A}{2p^2(\mu-1)}\left(\frac{R}{R_0}\right)^{-2(\mu-1)} + \ldots\right\} && ;\mu > 1 \end{aligned}\right\} \tag{4.3}$$

with

$$\Delta' = \Delta'_0\left(\frac{V_0}{V}\right) \tag{4.4}$$

where (R_0, V_0), the initial values of (R, V), have been introduced to ensure that all the constants $\tilde{\beta}$, $\tilde{B}$, α, and A are dimensionless. The aspect ratio behaves as

$$\left.\begin{aligned} \left(\frac{H}{R}\right) &= \beta\left(\frac{R}{R_0}\right)^{-(2-2\alpha)} && ;\mu \leqslant 1 \\ &= B\left\{\left(\frac{R}{R_0}\right)^{-3} - \frac{A}{2p^2(\mu-1}\left(\frac{R}{R_0}\right)^{-(1+2\mu)} + \ldots\right\} && ;\mu > 1 \end{aligned}\right\} \tag{4.5}$$

where

$$\beta = \tilde{\beta}H_0/R_0\,; \qquad B = \tilde{B}H_0/R_0 \tag{4.6}$$

The large time (large R) behaviour of the other variables is conveniently written in terms of that of U and of (H/R). We find

$$\left.\begin{aligned} W &= 2\alpha\left(\frac{H}{R}\right)U && ;\mu\leqslant 1 \\ &= \alpha_{\mathrm{T}}\left[\gamma\frac{H}{R}\right]^{1+2(\mu-1)/3} U && ;\mu>1 \end{aligned}\right\} \tag{4.7}$$

$$\left.\begin{aligned} k &= \left(\frac{2\alpha}{\alpha_{\mathrm{T}}}\right)^{2\lambda} p^{2\lambda-2}\left(\frac{H}{R}\right)^{2\lambda} U^2 && ;\mu\leqslant 1 \\ &= \left[\gamma\frac{H}{R}\right]^{2/3} U^2 && ;\mu>1 \end{aligned}\right\} \tag{4.8}$$

and

$$\left.\begin{aligned} Ri &= \left(\frac{2\alpha p}{\alpha_{\mathrm{T}}}\right)^{-2\lambda}\left(\frac{H}{R}\right)^{-2\lambda} && ;\mu\leqslant 1 \\ &= \left[\gamma\frac{H}{R}\right]^{-2/3} && ;\mu>1 \end{aligned}\right\} \tag{4.9}$$

there we have defined

$$\lambda=(1+2\mu)^{-1} \tag{4.10}$$

and

$$\gamma=\alpha_{\mathrm{f}}p^5/\alpha_{\mathrm{D}}\kappa^4 \tag{4.11}$$

In each case the shape factor s is asymptotically constant

$$s=(p/\kappa)^2 \tag{4.12}$$

Finally the independent constants α, β, A, B, and p introduced in the solution are constrained to satisfy

$$\left.\begin{aligned} \frac{p^2(4-\kappa^2)}{\kappa^2} &= 4-2\alpha p^2 && ;\mu\leqslant 1 \\ &= 1 && ;\mu>1 \end{aligned}\right\} \tag{4.13}$$

$$\left.\begin{aligned} \alpha_{\mathrm{f}}\left(\frac{p}{\kappa}\right)^4 + \frac{\xi_1}{4}(2\alpha p^2) &= \alpha && ;\mu<1 \\ &= \alpha\left(1+\frac{2\alpha_{\mathrm{D}}}{\alpha_{\mathrm{T}}}\right) && ;\mu=1 \\ \alpha_{\mathrm{f}}\left(\frac{p}{\kappa}\right)^4 &= \frac{\alpha_{\mathrm{D}}}{pB}\left(\frac{AB}{p\alpha_{\mathrm{T}}}\right)^{3\lambda} && ;\mu>1 \end{aligned}\right\} \tag{4.14}$$

4.3 The role of the parameter μ

The asymptotic solution for $\mu > 1$ is manifestly very different from that with $\mu \leqslant 1$. (Note that the $\mu = 1$ results here are not recovered simply by taking the limit $\mu \to 1$ in the $\mu > 1$ solution as it is not permissible to interchange the limits $\mu \to 1$ and $R \to \infty$.) The critical nature of the point $\mu = 1$ is illustrated by looking at the relative importance of the buoyant destruction (B.D.) and dissipation (DISS.) terms in the turbulence eqn. (3.11). We readily find

$$\frac{\text{B.D.}}{\text{DISS.}} = \frac{\alpha_T}{2\alpha_D} \frac{1}{(1+\Delta')} (Ri)^{1-\mu} \tag{4.15}$$

Therefore, for large Richardson number, this ratio is determined crucially by the value of μ. For $\mu < 1$ buoyant destruction dominates dissipation as the mechanism for removing turbulent energy. For $\mu = 1$ they are of the same order of magnitude (independent of the Richardson number). For $\mu > 1$ the entrainment is sufficiently suppressed that dissipation dominates buoyant destruction. In fact for $\mu > 1$ the entrainment suppression is sufficient to stop all entrainment at large time (as Ri defined in eqn. (3.4) becomes large) resulting in a cloud of finite, non-zero concentration. This has not been observed (even if it were the true situation, one would need to follow a dense cloud for a long time in absolutely calm conditions to demonstrate it experimentally) and we shall not pursue the $\mu > 1$ case further here.

4.4 The solution for $\mu \leqslant 1$

For $\mu \leqslant 1$, the qualitative nature of the solution is not strongly dependent* on μ. It resembles the simple model of Section 1 with Froude number p and "edge-entrainment" coefficient α, which are related to the input parameters α_f, K, ξ_1, α_D, and α_T via eqns. (4.13) and (4.14).

This is particularly remarkable in view of the entrainment model in eqns. (3.1–3.4) which is quite different in appearance from that of Section 1. It is well known [4,13] that the model in eqn. (3.1) cannot conserve energy if $W \sim U$. By imposing conservation of energy we have obtained eqn. (4.7), which (for $\mu \leqslant 1$) is responsible for the similarity between the results of this model and that of Section 1. Note also from eqn. (4.8) that the turbulence intensity is not simply proportional to U^2, but also has a factor dependent on the evolution of the aspect ratio.

Neither of the parameters α or p depends upon the initial aspect ratio H_0/R_0. This gives a behaviour $\tilde{\beta}^{-1} t^{-\alpha}$ of the mean concentration with universal α, irrespective of the initial cloud, and answers in part the question we set out to investigate.

The asymptotic analysis, however, does not give any information about $\tilde{\beta}$ (the value of which depends upon the dilution process, and therefore upon the

*Not even for the case $\mu = 0$ where there is no suppression of entrainment.

level of turbulence, during the initial, radially accelerating phase). Nor does it indicate (without being carried further) how rapidly the asymptote is approached. One might, for example, expect the Boussinesq approximation, on which the asymptotic analysis relies, to become valid later for denser clouds and hence give a slower approach to the asymptote.

4.5 Numerical solution for $\mu = 1$

To examine the solution further, we have obtained numerical solutions for the case $\mu = 1$ with various values of the other input parameters. Comparison of the asymptotic solution with Thorney Island results guides our choice of input parameters. In particular we shall demand $p = 1$, $\alpha = 0.7$ [6–8]. Thus eqns. (4.13) and (4.14) require

$$\left.\begin{aligned} \kappa &= 1.054 \\ \frac{\alpha_f}{(2-\xi_1+4\alpha_D/\alpha_T)} &= 0.43 \end{aligned}\right\} \qquad (4.16)$$

By taking $\kappa = 1.054$ and choosing α_f, ξ_1, α_D, and α_T to satisfy eqn. (4.16) we can thus investigate the dependence of the results on the initial density, the initial aspect ratio, as well as on the degrees of freedom in the choice of α_f, ξ_1, α_D, and α_T.

To investigate the dependence of Δ_0' we specify* $\alpha_f = 0.5$, $\alpha_D = 1.45$, $\alpha_T = 5.0$, $\xi_1 = 2.0$ and take $\Delta_0' = 0.1$, 1.0, and 2.0. The results bear out the asymptotic analysis. In Fig. 1a we have plotted dimensionless radius against dimensionless time**.

The radial behaviour $R_*(t_*)$ is almost completely independent of Δ_0' and such dependence as there is confined to early times ($t_* \leqslant 10$). The volume (or alternatively the concentration $C_* = V(0)/V$, see Fig. 1b) has the calculated asymptotic behaviour (see eqn. (4.3) and thereafter) and the numerical results give $\tilde{\beta} = \beta R_0/H_0 \approx 0.9$ for these cases, but the convergence to the asysymptote is rather slower than for $R_*(t_*)$ for each of the values of Δ_0'.

Figure 1c shows $k_*(t_*)$ for which the asymptote is now exactly specified by

*These values of (α_f, α_D, α_T, and ξ_1) are of the expected order of magnitude and satisfy eqn. (4.16). The choice is otherwise arbitrary. We discuss the sensitivity of α_D and α_T below but do not attempt to explore the whole 3-dimensional parameter space of values satisfying eqn. (4.16).

**Dimensionless variables are defined by $R_* = R/R_0$, $U_* = U/U_0$, $C_* = V_0/V$, $k_* = k/U_0^2$, $t_* = t/t_0$, where $U_0 = (g\Delta_0' H_0)^{1/2}$, and R_0, V_0, H_0, Δ_0' are initial values of the respective variables, and $t_0 = R_0/U_0$. The choice of these scales is not entirely arbitrary, but rather ensures that the simple model of Section 1 relates dimensionless variables independently of H_0/R_0 and Δ_0'. furthermore in plots with time as the abscissa we have used $1 + 2t_*$ because the model of Section 1 has $R_*^2 = 1 + 2t_*$ (for unit Froude number). Deviations from a linear behaviour on a log-log plot therefore give a measure of the effect of the initial acceleration régime.

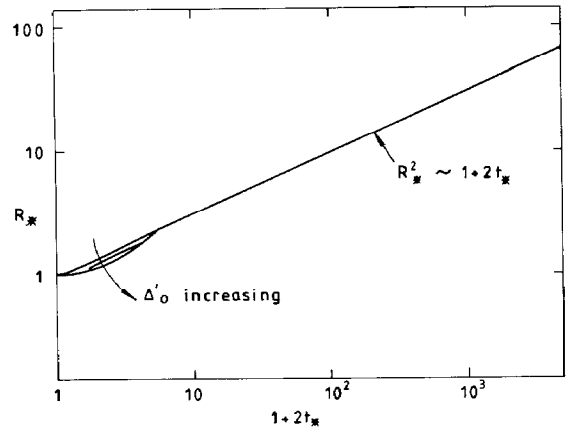

Fig. 1a. (Dimensionless) radius as a function of dimensionless time. The initial cloud density has little effect. Curves for $\Delta'_0 = 0.1$, 1.0, and 2.0 are shown. Note that the time-scale depends on Δ'_0 and so the curves will appear different if dimensioned time is used.

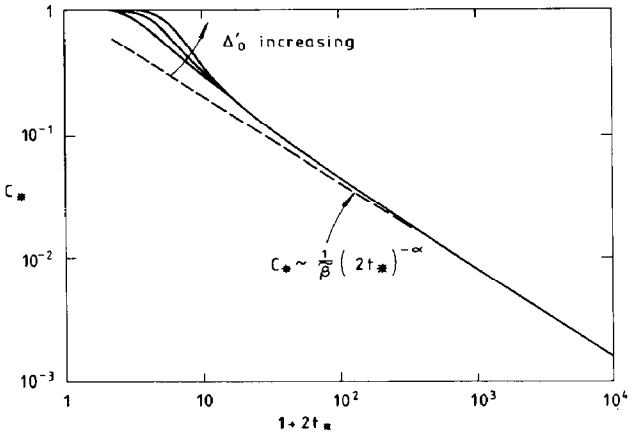

Fig. 1b. Concentration as a function of dimensionless time for $\Delta'_0 = 0.1$, 1.0, and 2.0. Increased inertia causes a slight delay in entrainment.

eqn. (4.8) using the value of β obtained from the concentration. Convergence to the asymptote is rapid. There is significant dependence on Δ'_0, but only in the initial, radially accelerating phase where the turbulent kinetic energy density is increasing rapidly. The behaviour of the shape factor s (Fig. 1d) shows that the initial density-dependent phase, seen in the previous figures, is associated with the régime where the cloud has not yet settled into a self-similar flow. When such a flow is established, s is constant and there are no remaining density effects, although a higher initial density does delay, slightly, the onset of self-similar flow.

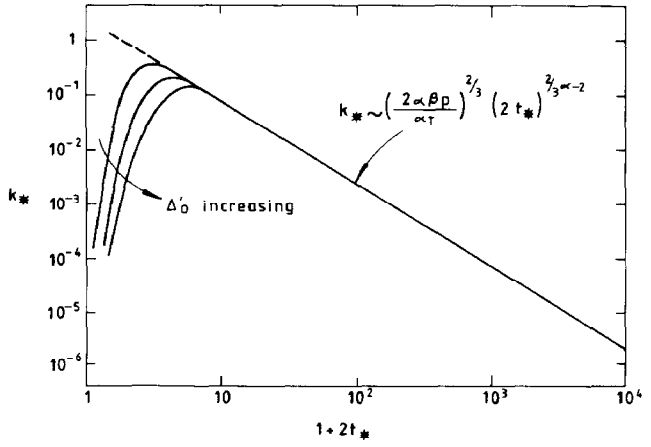

Fig. 1c. Dimensionless turbulent kinetic energy density as a function of dimensionless time for $\Delta_0' = 0.1$, 1.0, and 2.0. Increased inertia delays convergence to the asymptote given in Section 4.4.

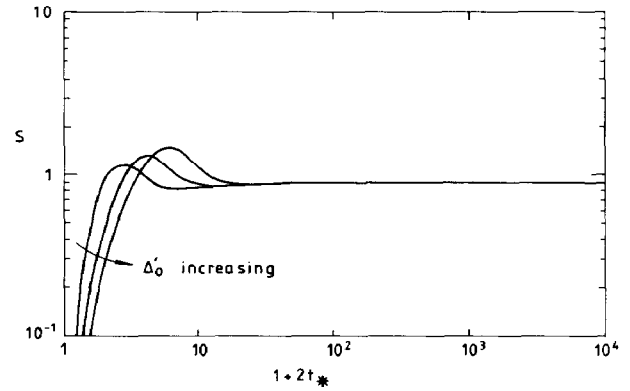

Fig. 1d. The shape factor as a function of dimensionless time.

In Figs. 2a and 2b we show results for $(\alpha_T, \alpha_D) = (0.5, 0.145)$ compared with $(\alpha_T, \alpha_D) = (5, 1.45)$ with $\Delta_0' = 0.1$ and the other parameters as above. These results show that the fixed ratio α_T/α_D does indeed imply the same slope of the asymptotes of $V_*(t_*)$, and $k_*(t_*)$ as shown in the analysis of Section 4.2. The value of $\tilde{\beta}$ however depends on α_T, being 1.44 and 0.9 for the respective cases. Early on, the lower value of α_T causes less entrainment and higher concentrations. However, at large time the higher level of turbulence correspond-

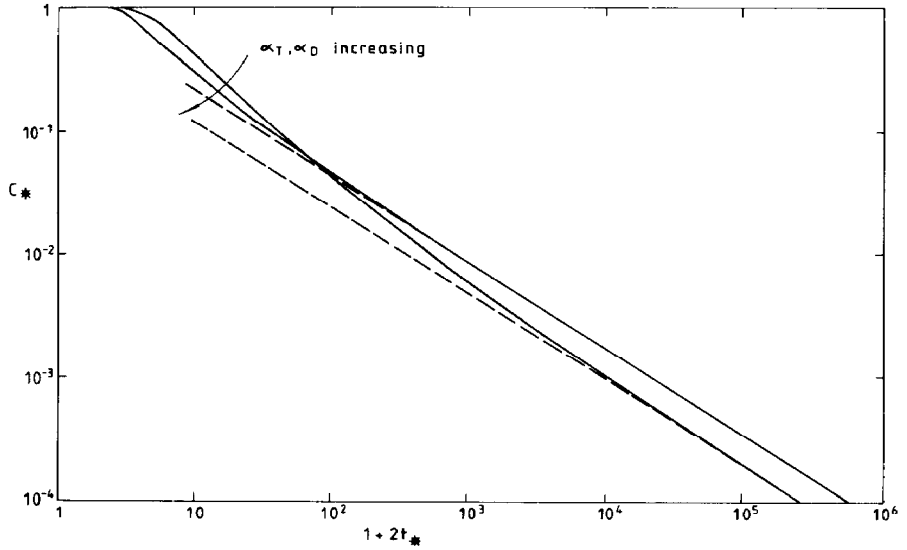

Fig. 2a. Concentration as a function of dimensionless time for different values of α_T with α_T/α_D fixed. The asymptotes are parallel. Smaller α_T/α_D measures slower convergence to a lower asymptote.

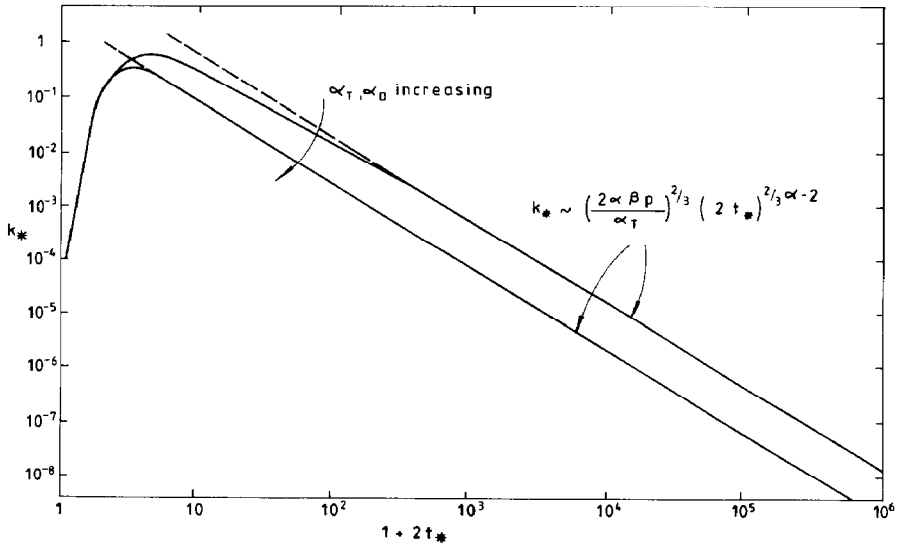

Fig. 2b. Turbulent kinetic energy as a function of dimensionless time for different values of α_T with α_T/α_D fixed.

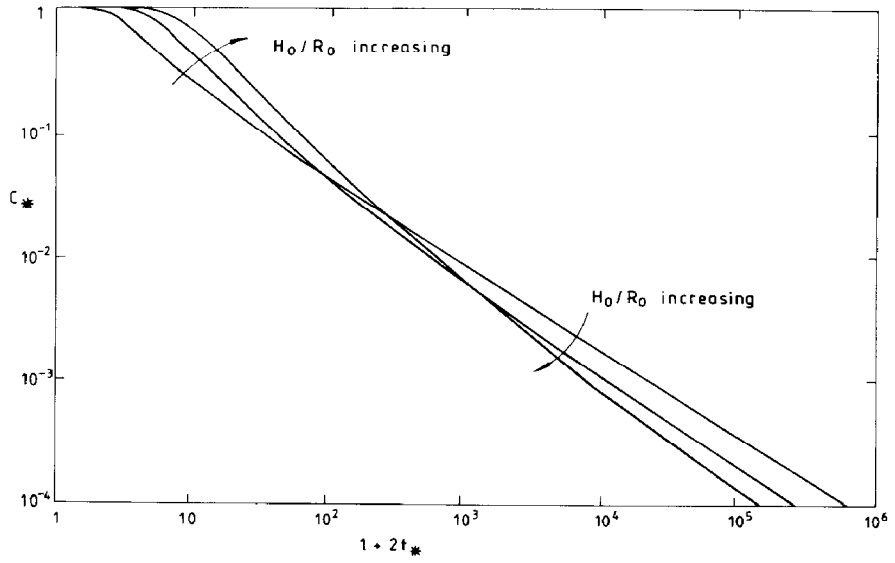

Fig. 3a. Concentration as a function of dimensionless time for different aspect ratios $H_0/R_0 = 10.7$, 2, and 0.1. The asymptotes are parallel with more rapid convergence to the asymptote for small H_0/H_0.

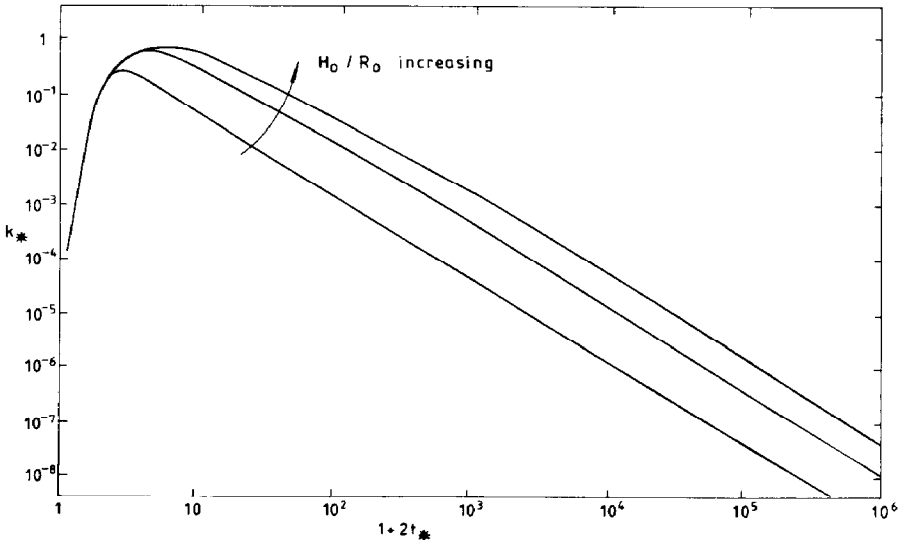

Fig. 3b. Turbulent kinetic energy as a function of dimensionless time for different aspect ratios. Higher initial aspect ratio gives a higher (dimensionless) turbulent energy.

ing to the lower values of α_T and α_D causes more entrainment and hence lower concentrations*. Hence the different values of $\tilde{\beta}$. It is interesting to note that $\tilde{\beta}$ may lie either side of the value 1.0 which is implied by the simpler models discussed in the introduction.**

In Figs. 3a and 3b we compare results for different values of the initial aspect ratio. We take*** $H_0/R_0 = 10.7$, 2 and 0.1. Other parameters are $\Delta_0' = 0.1$ and $(\alpha_T, \alpha_D) = (0.5, 0.145)$, and the rest as previously. All the results are consistent with the asymptotic analysis of Section 4.2. However, $\tilde{\beta}$ depends on the initial aspect ratio. Furthermore, convergence of the concentration C_* to the asymptote is very slow for large initial aspect ratio H_0/R_0. For higher initial aspect ratio the initial dilution is less, but subsequently a higher level of turbulence (as a result of the larger initial potential energy) results in lower asymptotic concentrations. The effects on the concentration of varying α_T, with α_T/α_D fixed, and of varying H_0/R_0 are summarised in Figs. 4a and 4b. The concentration is proportional to $\tilde{\beta}^{-1}$ and the (dimensionless) turbulent kinetic energy to $(\beta/\alpha_T)^{2/3}$.

4.6 Early-time concentration records from experiments

In most of the Thorney Island trials, the concentration sensors were placed sufficiently far away from the source that the initial effects discussed in this work were not observed. However, in a few trials there were sensors close to the source. Figure 5 shows area-averaged concentration as a function of dimensionless time for four such trials. The straight line is $C_* = (1+2t_*)^{-0.7}$, which is found to give a good approach to the onset of the concentration data (that is from the release to the time when the first sensor was reached) over the whole set of Phase I trials [14]. There is some evidence that the denser releases lie higher in Fig. 5 than the less dense ones, and we claim qualitative agreement**** with the results of our model, shown in Fig. 1b.

Whilst the Thorney Island trials were all conducted with essentially the same initial aspect ratio, small scale calm-air experiments have been performed at different aspect ratios by Havens and Spicer [15,16]. In their data there is some evidence [15] that the value of $\tilde{\beta}$ in the asymptotic behaviour $C_* \sim \tilde{\beta}(2t_*)^{-\alpha}$ may depend on the aspect ratio, but the effect, if present, is small.

---

*Note that whilst more turbulent energy tends to encourage more entrainment, the higher rate of entrainment also absorbs more turbulent energy as a source of power. In the case where α_D and α_T are altered in proportion, then, at sufficiently large time, the latter effect is predominant and smaller α_T corresponds to higher levels of turbulence.

**The concentration behaves asymptotically as $\tilde{\beta}^{-1}(R/R_0)^{-2\alpha}$.

***This takes the model beyond the region where its "shallow-layer" derivation is valid but does demonstrate the relative insensitivity to H_0/R_0!.

****In view of the simplicity of our shallow-layer derived model we cannot really expect more than this and do not therefore attempt a detailed fit.

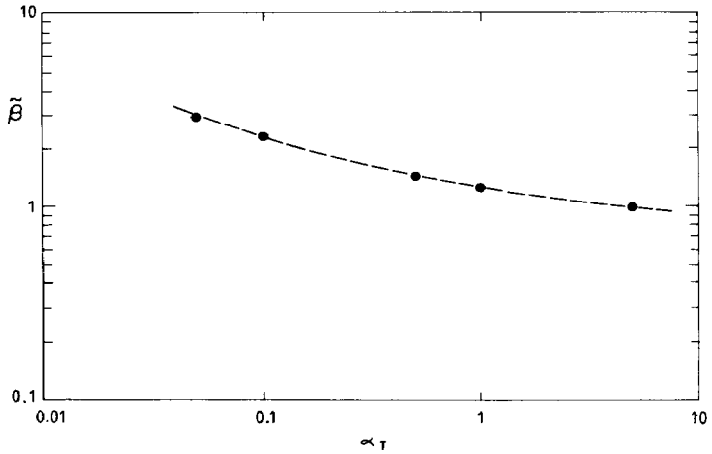

Fig. 4a. Variation of $\tilde{\beta}$ with α_T for fixed α_T/α_D.

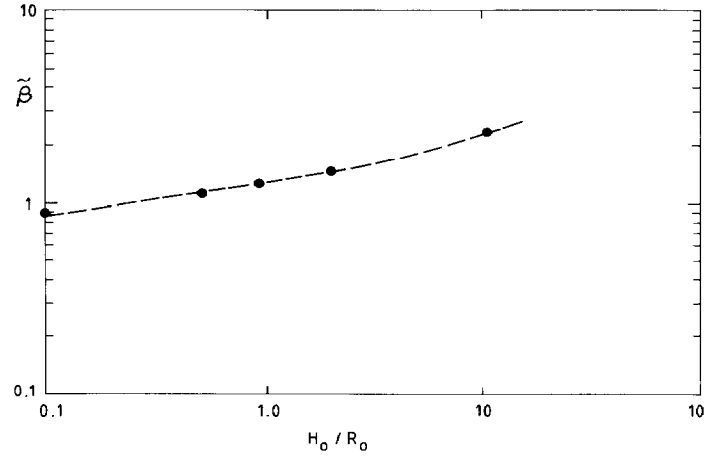

Fig. 4b. Variation of $\tilde{\beta}$ with initial aspect ratio.

4.7 Further comments

Two other recent works deserve comment.

First, the question of how entrainment is affected by the initial aspect ratio of the cloud has been addressed by Fay and Zemba [17]. In a comparison with wind tunnel data [18] they conclude that gravity driven entrainment is much less for clouds of low initial aspect. This, however, is misleading and stems from a somewhat ad hoc choice of entrainment model. In calm conditions, where top entrainment is absent, their model simply takes a constant volume increase rate given by

$$\frac{dV}{dt} = k_{FZ} V_0^{2/3} \ (g\Delta_0' V_0^{1/3})^{1/2} \tag{4.17}$$

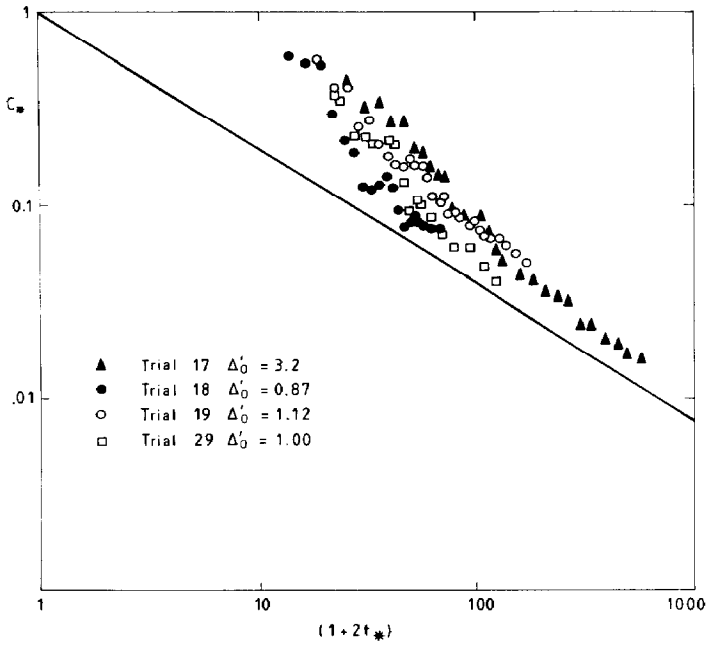

Fig. 5. Area averaged concentration at a height of 0.4 m from the Thorney Island trial data including sensors near the source. (Preliminary analysis.)

where V_0 and Δ'_0 are initial values of V and Δ', and k_{FZ} is a constant. The solution of eqn. (4.17) may be written as

$$\frac{V}{V_0}=\left[1+\pi^{-1/6}k_{FZ}\left(\frac{R_0}{H_0}\right)^{2/3}\frac{t}{t_0}\right] \tag{4.18}$$

in order to compare it with the model of Section 1:

$$\frac{V}{V_0}=\left[1+2\kappa\frac{t}{t_0}\right]^{\alpha_E} \tag{4.19}$$

where

$$t_0=R_0^2/\sqrt{b} \tag{4.20}$$

Fay and Zemba observe that $k_{FZ}=0.6$ provides a good fit to data of high initial aspect ratio but that this value is too large to fit low aspect ratio data. However, our comparison of eqns. (4.18) and (4.19) between models indicates (irrespective of the difference in power law) that constant α_E would correspond more closely to $k_{FZ}\sim(H_0/R_0)^{2/3}$. In the context of the model presented here, then, we should expect k_{FZ} to be smaller for low initial aspect ratio. We thus find that Fay and Zemba's result is quite consistent with constant α_E. Ref.

[17], then, provides no grounds to suppose that the widely used edge entrainment model of Section 1 will not be appropriate to low aspect releases.

Second, a very similar model to that derived in Sections 2 and 3 has very recently been considered by van Ulden [19]. He has introduced more detailed modelling of the turbulence production mechanisms and the forces on the cloud. To compare his method with ours let us note that the gravity term in our spreading eqn. (3.8) may be expanded by substituting for the shape factor s from eqn. (3.7) to give

$$4g\ (\rho-\rho_a)(1-s)H/R=4g\rho_a\Delta' H/R-\frac{4}{\kappa^2}\rho_a\ U^2/R \tag{4.21}$$

The terms on the left represent gravity and front-resistance forces directly analogous to those given in Ref. [19]. The coefficients of the terms are slightly different owing to the different depth profiles assumed: we take the parabolic profile of the shallow self-similar solution in the limit of no entrainment; van Ulden (see also Ref. [20]) takes a uniform profile. The structure of the equations, however, is the same in the shallow ($H/R \ll 1$) limit. For an accurate description of "deep" clouds one would in general expect "correction" terms of higher order in (H/R). Van Ulden's model has these and he has demonstrated a good fit to experimental data. Furthermore, his results are qualitatively consistent with ours, and we thus regard his work as giving added support to our own conclusions.

5. Discussion and conclusions

5.1 Summary

We have presented an integral model for a heavy gas cloud spreading in calm conditions. In contrast to previous such models, it treats the turbulent energy within the cloud as an independent, dynamic variable and relates the entrainment rate to this. It does this in such a way that dissipation of mechanical energy is guaranteed. This has allowed us to study the dependence of the dilution process on the initial density and on the initial aspect ratio. This study sheds light on the validity of simpler models for the early phases of dilution, in particular for initial conditions not currently covered by field trials.

5.2 Entrainment

Entrainment into the top of the cloud is assumed to be related to the turbulence intensity by a factor proportional to $Ri^{-\mu}$.

If $\mu > 1$, then this suppression factor is sufficient, eventually, to stop all entrainment as an asymptotically constant concentration is reached. In the absence of any experimental evidence for this, we therefore reject this case. (However, technically one can only look for an upper bound for μ dependent on how long one can follow an experiment in absolutely calm conditions.)

If $\mu \leqslant 1$ then the resultant entrainment appears very similar to the standard edge entrainment model [3,4] discussed in the introduction. A significant difference is that the effective edge entrainment coefficient α is not an input parameter to the calculation and the derived value may depend on the initial density difference Δ_0', and the initial aspect ratio H_0/R_0. In fact (in the $\mu=1$ model which we have analysed in some detail) it turns out to depend on neither of these; the concentration goes asymptotically as $t^{-\alpha}$ for a universally constant α. However, the coefficient of $t^{-\alpha}$ does depend on H_0/R_0 (but hardly at all on Δ_0' in the range considered) and the approach to the asymptote may be so slow for large H_0/R_0 that the concentration may descend more steeply than $t^{-\alpha}$ over a number of orders of magnitude in time. The size of this effect also depends on the coefficients of the terms involving dissipation and buoyant destruction of energy which may be altered in proportion without affecting the exponent α.

The fact that the concentration approaches the $t^{-\alpha}$ asymptote from above is a natural consequence of the smaller entrainment rate in the radial acceleration phase where the mean kinetic energy is building up. To see this explicitly, consider the simple model defined by $\mathrm{d}R/\mathrm{d}t = U_\mathrm{f}$, $\mathrm{d}V/\mathrm{d}t = (2\pi RH)\,U_\mathrm{E}$, $H = V/\pi R^2$, and $U_\mathrm{E} = \alpha U_\mathrm{f}$. It is straightforward to see that $(V/V_0) = (R/R_0)^{2\alpha}$ in this model irrespective of the definition of U_f. Thus the small-time behaviour of R translates directly into the small-time behaviour of the concentration, and radial acceleration implies concentration decreasing to the asymptote. However, whilst this simple model gives a universal curve $C(R_*)$ independent of initial conditions, the more complicated, dynamic-turbulence model does not. We thus distinguish these two aspects of the model: on the one hand U_E increases with U_f in the acceleration phase, but on the other, the structure of the turbulence model means that this is not in direct proportion.

Overall we regard the results for entrainment as lending considerable support to the simpler models which take an "edge entrainment" proportional to U_f. Some models have made other assumptions, such as taking a "top entrainment" proportional to U_f (see Refs. [3–5] for a review). Our results show how a consideration of the energy budget comes down strongly in favour of the edge-entrainment models (but of course do not rule out top entrainment in the régime where "atmospherically-powered" turbulence dominates "cloud-powered" turbulence).

5.3 Buoyant destruction and dissipation of turbulence

These terms are of the same order only in the $\mu=1$ model (see Section 4.2). If μ is less than 1 then buoyant destruction dominates. These results contrast with mixing box experiments where turbulence is created away from the density interface and dissipation is dominant typically by a factor of 10:1, over buoyant destruction [3]. We believe that this contrast lends support to the view that entrainment into heavy gas clouds spreading in calm conditions arises

principally owing to the turbulence created close to the density interface from the interaction between the spreading cloud and the ambient air; intuitively, turbulence generated close to the density interface should power entrainment more readily than turbulence created away from the density interface, and thus one may expect a higher ratio of buoyant destruction to dissipation in spreading gas clouds than in mixing box experiments. Further, in the integral model we have treated the turbulence as averaged over the whole of the cloud, but should the turbulence causing entrainment be primarily at the edge, as suggested above, then we assume the difference can be absorbed into the value of α_T. Consequently there is no reason to suppose that α_T in our model should have a value close to that found in mixing box experiments.

5.4 The turbulence intensity

It is interesting to note that the turbulence intensity in the cloud in this model, given by eqn. (4.21) is not simply $k \sim U^2$, nor does it correspond to any simple model of turbulent energy near the front being averaged over the whole cloud volume. Thus the model serves to illustrate that even if a simple integral model fits data on entrainment and spreading, one should be very wary of drawing simple conclusions about the level of turbulence in the cloud; the dynamics of turbulence make the relationship between turbulent and entrainment velocities a complicated one.

5.5 Conclusions

The model presented here admits the possibility of a dependence of the dimensionless concentration function C on the initial aspect ratio and on the initial relative density. The concentration goes asymptotically as $\tilde{\beta}^{-1}(2t_*)^{-\alpha}$ where $\tilde{\beta}$ depends on the initial conditions but α does not. The rate at which the concentration tends to this asymptote (from above) also depends upon the initial conditions and, in particular, for large aspect ratios may be slow, giving a steeper behaviour than $t_*^{-\alpha}$. However, over the parameter range we have considered, these effects are small (involving typically no more than a factor 2 in concentration, even close to the source). In fact in areas of practical interest the results of the model resemble those of the much simpler edge entrainment model discussed in the introduction, where α is assumed independent of the initial density and aspect ratio.

Our conclusions are therefore as follows:

We do not expect a large variation of concentration at given t_* with the initial density or with the aspect ratio of the release. There is some evidence for this conclusion in existing data but more complete verification would be desirable. If, therefore, it is not necessary (from the hazard analysis viewpoint) to model such effects, then it is adequate to return to the simpler models where edge entrainment is assumed proportional to the front velocity. The analysis presented here lends considerable support to this approach.

Our model is complemented by that of van Ulden [19–21] which fits into the same framework: our results indicate why a simple model with constant entrainment coefficient α independent of initial conditions may be adequate for most hazard analysis purposes; van Ulden's results show that a model of the same structure, if extended to contain terms of higher order in H/R may fit high aspect ratio data accurately.

The other effect highlighted in this work is the general deviation of the concentration at early times from the asymptotic $t^{-\alpha}$ behaviour. Such behaviour can, if desired, be produced in a model with the "traditional" edge entrainment assumption, $U_E = \alpha U_f$, if radial acceleration effects are considered in modelling U_f. However, it remains to be seen whether such an approach could give more than a qualitative reproduction of data such as that in Fig. 5.

Our model indicates that "top entrainment", in the framework of Section 1, need not be considered in calm conditions (whether air enters through the top or elsewhere is a different question) and those models which introduce it to the extent that they violate conservation of energy (see Refs. [3,4,13] for a review) are ruled out.

Acknowledgements

The authors would like to thank Dr. P.W.M. Brighton for the data shown in Fig. 5, which result from a preliminary analysis of the individual concentration records.

The work reported in this paper was carried out under contract for the Health and Safety Executive and forms part of an overall programme of research and development relating to safety and reliability.

References

1 J. McQuaid and B. Roebuck, Large scale field trials on dense vapour dispersion, Report EUR 10029 EN, Commission of the European Communities, Brussels, 1985.

2 J. McQuaid, Objectives and design of the Phase I Heavy Gas Dispersion Trials, J. Hazardous Materials, 11 (1985) 1–33.

3 C.J. Wheatley and D.M. Webber, Aspects of the dispersion of denser-than-air vapours relevant to gas cloud explosions, Report EUR 9592 EN, Commission of the European Communities, Brussels, 1984.

4 D.M. Webber, The physics of heavy gas cloud dispersal, UKAEA Report SRD R 243, Safety and Reliability Directorate, Culcheth, Warrington, Great Britain, 1983.

5 D.M. Webber, Gravity spreading in dense gas dispersion models, In: G. Ooms and H. Tennekes (Eds.), Atmospheric Dispersion of Heavy Gases and Small Particles, Springer, 1984.

6 A.J. Prince, D.M. Webber and P.W.M. Brighton, Thorney Island Heavy Gas Dispersion Trials – Determination of path and area of cloud from photographs, UKAEA Report SRD R 318, Safety and Reliability Directorate, Culcheth, Warrington, Great Britain, 1985.

7 P.W.M. Brighton, A.J. Prince and D.M. Webber, Determination of cloud area and path from visual and concentration records, J. Hazardous Materials, 11 (1985) 155–178.

8 P.W.M. Brighton, Area-averaged concentrations, height-scales and mass balances, J. Hazardous Materials, 11 (1985) 189–208.
9 R.G. Picknett, Dispersion of dense gas puffs released in the atmosphere at ground level, Atm. Environ., 15 (1981) 500–525.
10 J.E. Simpson and R.E. Britter, Experiments on the dynamics of the front of a gravity current, 2nd IAHR Symposium on Stratified Flows, Trondheim, Tapir Press, 1980.
11 D.M. Webber and P.W.M. Brighton, A mathematical model of a spreading vaporising liquid pool, In: S.H. Hartwig (Ed.), Heavy Gas and Risk Assessement III, Reidel, 1986, pp. 223–232.
12 D.M. Webber and P.W.M. Brighton, Inviscid similarity solutions for slumping from a cylindrical tank, J. Fluids Eng., 108 (1986) 238–240.
13 J.A. Fay, Some unresolved problems of LNG vapour dispersion, In: J.A. Havens (Ed.), Proc. MIT/GRI LNG Safety and Research Workshop, Report GRI 82/0019.2, Gas Research Institute, Chicago, 1982.
14 C.J. Wheatley, A.J. Prince and P.W.M. Brighton, Comparison between data from the Thorney Island heavy gas trials and predictions of simple dispersion models, UKAEA Report SRD R355, Safety and Reliability Directorate, Culcheth, Warrington, Great Britain, 1986.
15 J.A. Havens and T.O. Spicer, Gravity spreading an air entrainment by heavy gases instantaneously released in a calm atmosphere, In: G. Ooms and H. Tennekes (Eds.), Atmospheric Dispersion of Heavy Gases and Small Particles, Springer, 1984.
16 J.A. Havens and T.O. Spicer, Development of an atmospheric dispersion model for heavier than air gas mixtures, Vol. II (Laboratory Calm Air Heavy Gas Dispersion Experiments), US Coast Guard Report CG-D-23-85, 1985.
17 J.A. Fay and S.G. Zemba, Dispersion of initially compact dense gas clouds, Atmos. Environ., 19 (1985) 1257–1261.
18 D.J. Hall, Further experiments on a model of an escape of heavy gas, Report LR(312) AP, Warren Spring Laboratory, Stevenage, Herts, Great Britain, 1979.
19 A.P. van Ulden, Heavy gas dispersion in still air, Presented at the IMA Conference on Stably Stratified Flow and Dense Gas Dispersion, Chester, April 1986, Oxford University Press, 1987, in press.
20 A.P. van Ulden, A new bulk model for dense gas dispersion: two-dimensional spread in still air, in: G. Ooms and H. Tennekes (Eds.), Atmospheric Dispersion of Heavy Gases and Small Particles, Springer, 1984.
21 A.P. van Ulden, The heavy gas mixing process in still air at Thorney Island and in the laboratory, J. Hazardous Materials, 16 (1987) 411–425.